

QUANTIFYING DEPTH UNCERTAINTY: A GEOSTATISTICAL VELOCITY AND ANISOTROPY ANALYSIS OVER THE PETREL FIELD, AUSTRALIA

K. Dancer¹, G. Byerley², F. Renard², P. Woods³, T. Rayment¹

¹ DUG Technology; ² Neptune Energy Group Holdings; ³ Neptune Energy Bonaparte Pty Ltd

Summary

The Petrel gas field is situated 200 km offshore north-western Australia. One of the biggest uncertainties in the field gas initially in place (GIIP) estimates has been the presence of a very low relief spill point, and whether the field closes in a way that reconciles with the free water level interpreted from well log analysis, pore pressure and dynamic data. A modern 3D seismic survey was acquired and processed to better image the target reservoir and structure. Following this, the structural uncertainty of the top reservoir and closure was quantified, enabling better GIIP estimates. The prime contributors to the depth uncertainty are identified, then the spatial characteristics of the velocity are used to derive variograms, which are subsequently used to generate many velocity realisations. Analysis of these provides quantitative estimates of the structural uncertainty and its impact on the in-place volume of gas. Inconsistency between the most likely well derived free water level ranges and the P50 lowest closing contours estimated from this study has challenged the previous interpretation of a fully closing four-way dip closure as the main trapping mechanism, while a conventional structural trap remains a possibility.

Quantifying depth uncertainty: A geostatistical velocity and anisotropy analysis over the Petrel field, Australia

Introduction

The Petrel gas field is situated 200 km offshore north-western Australia in the Bonaparte Basin. The reservoir consists of Permian Cape Hay sandstones with the crest of the field at a depth of around 3520 m. The field was initially identified as a large four-way dip closure delineated by a 2D seismic campaign in the 1960s. The first discovery well was drilled into the crest of the structure in 1969. Since that time, an additional seven wells have been drilled by three different operators spanning from 1971 to 2011 with gaps up to fifteen years in between. These wells underwent extensive data acquisition campaigns which included coring, wireline logging and well tests. The reservoir can be seen in Figure 1.

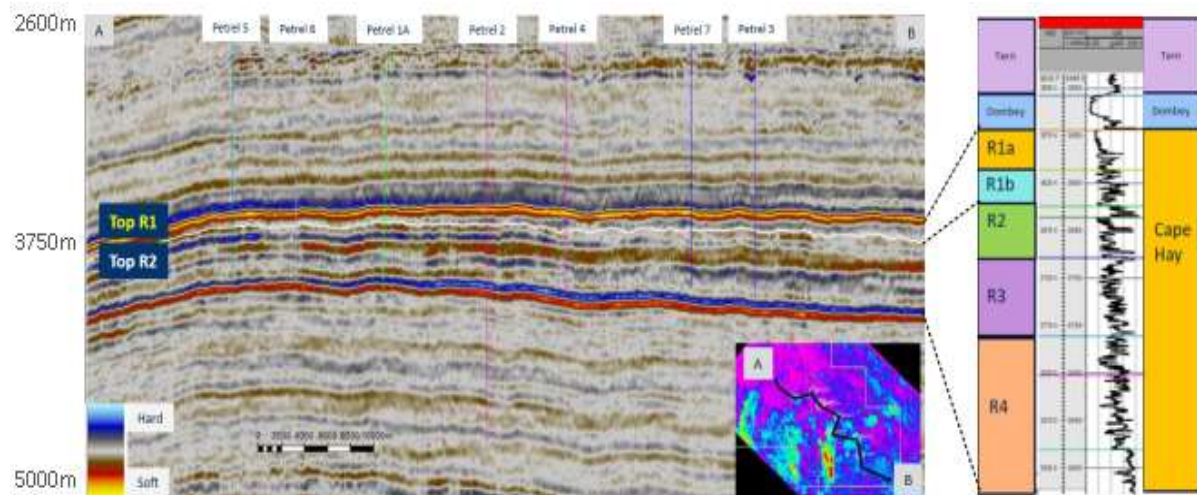


Figure 1 Top and base reservoir (Top R1 and Top R2) of the Petrel field, along a NW-SE arbitrary line going through the 7 Petrel wells. The spill point of the structure is located SE of Petrel-3 well.

One of the biggest uncertainties in the field gas initially in place (GIIP) estimates has been the presence of a spill point to the southeast of the field and whether or not the field closes in a way that reconciles with the free water level interpreted from well log analysis, pore pressure and dynamic data. Ideally, the lowest closing contour from the 3D seismic top reservoir depth map would support the presence of a simple four-way dip closure giving confidence in the trapping mechanism for the field. The spill point, however, is characterized by a very low relief structural saddle point which adds further uncertainty to the lowest closing contour and ultimately the resulting GIIP estimates of the field.

In 2019/20, a long offset, broadband, triple-source 3D seismic survey was acquired to better image the target reservoir and structure. The seismic processing and imaging workflow utilised the longer 8 km offsets to improve the velocity model away from well control using a combined full waveform inversion (FWI) and reflection tomography approach. Following this, the structural uncertainty of the top reservoir and closure was quantified, enabling better GIIP estimates. This paper describes the method used to analyse this uncertainty. The prime contributors to the depth uncertainty are identified, then the spatial characteristics of the velocity are used to derive variograms, which are subsequently used to generate hundreds of velocity realisations. These are then analysed, providing quantitative estimates of the structural uncertainty.

Initial earth model evaluation

The method presented relies on the existence of suitable imaging velocity and anisotropy (if relevant) models, evidenced by:

1. Flat common image gathers.

2. Vertical velocity (V_0) consistent with the check shot and sonic logs.
3. Horizon and well marker ties being accurate to within a reasonable tolerance.

The comprehensive TTI pre-SDM workflow, which included diving wave FWI to 12 Hz and five iterations of reflection tomography, ensured all criteria were met.

Given consistent gather-flatness, it is assumed that crosstalk between V_0 and the TTI anisotropic parameters are the most likely cause of uncertainty in V_0 , and hence the reservoir depths. In this workflow, we maintain the earth models at the well locations, where there is additional information to solve this crosstalk issue, and vary the models elsewhere. Where V_0 is updated, the anisotropic fields δ and ε are also updated such that the NMO velocity (V_{nmo}) and anellipticity η are kept constant, using formulae from Alkhalifah and Tsvankin (1995), preserving gather-flatness:

$$V_{\text{nmo}} = V_0 \sqrt{1 + 2\delta}, \quad (1)$$

$$\eta = \frac{\varepsilon - \delta}{1 + 2\delta}, \quad (2)$$

For this geological setting, it was considered unlikely that an interval would be consistently isotropic at the well locations yet anisotropic elsewhere in the survey area. Hence, inaccuracy in the models was most likely to be caused by crosstalk between anisotropy and velocity in the anisotropic layers. For this reason, the depth uncertainty focused on updating the velocity within three anisotropic layers while the isotropic layers were unchanged. However, it is also possible to use this approach to update the entire 3D model should there be sufficient justification to do so.

Variogram analysis

A variogram analysis is undertaken using information about the velocity field at the well locations where crosstalk between velocity and anisotropy is minimised. The spatial sampling of well information in this case allowed such an approach but for situations where well control is more limited, the seismic velocities themselves would be used for the variogram analysis.

Velocity trends are determined for each of the intervals being updated. The inclusion of trends in the variogram analysis can lead to an inaccurate estimate of the variogram parameters. For the i th well, the log-scalar ratio s_i between the interval velocity and the respective trend velocity is calculated:

$$s_i = \ln(V_i/V_i^{\text{trend}}), \quad (3)$$

where v_i is the average interval velocity within the layer at the location of the i th well, and v_i^{trend} is the trend-predicted interval velocity at that location. The variance between these log-scalars is plotted against the distance between the wells for each pair of wells.

Various variogram models were tested to determine which best described this data set, with a Gaussian variogram shape providing the best fit, as can be seen in Figure 2. This is unsurprising given the spatial consistency of the geology which was also evident during the velocity model building.

When selecting the variogram model to use for generating velocity realisations, both the geological setting and how well the model predicted the observed data are taken into account. A cost function is computed for each combination of model parameters (range and sill) and normalised so the model which best describes the data is set to 100% as exemplified by Figure 3. To generate the velocity realisations a subset of models is selected for each layer. For this project, a single range of 20 km was selected and the sill value varied from 50% to 150% of the sill that best fit the data for that range.

Velocity realisations

This subset of variogram models is used to generate hundreds of velocity realisations. For each realisation, one variogram model is selected per layer based on the relative likelihood of how well the model explained the observed data (depicted in Figure 2).

Once the variogram models are selected, realisations are generated using a turning bands algorithm which treats the realisation as a summation of cosine functions of varying frequencies (akin to plane waves), as described in Cressie (1993). The realisations are constrained to maintain the existing velocity profiles at the well locations, while maintaining the correct spatial statistics. This is achieved by kriging using the same variograms, again following Cressie (1993).

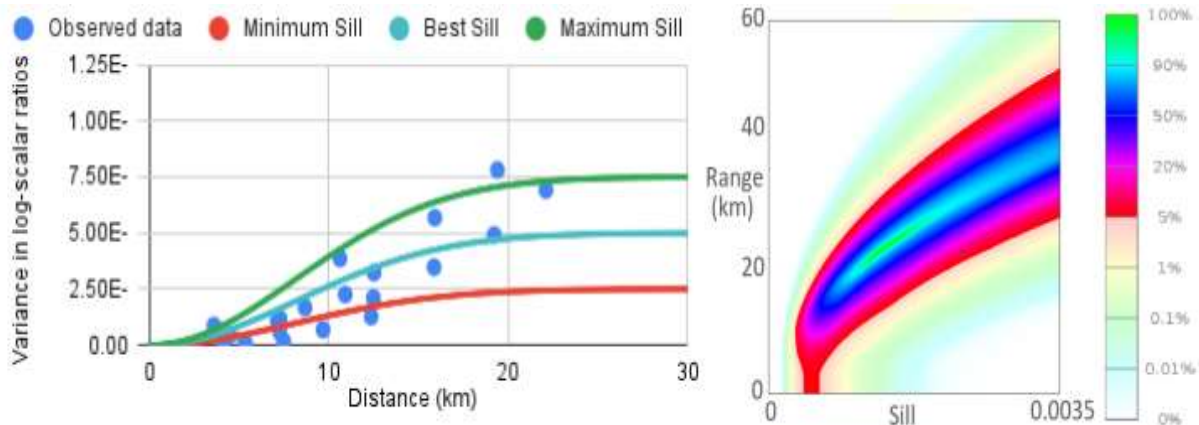


Figure 2 (left) Gaussian variograms for the third anisotropic layer of the chosen range, showing the best fit model and the spread of acceptable models. **Figure 3 (right)** Relative likelihood of Gaussian variogram models predicting the observed data for the third anisotropic layer.

For each realisation, the anisotropy fields are recalculated so that V_{nmo} and η are preserved according to equations (1) and (2). Only models with geophysically reasonable values of δ are accepted. In this case, 500 realisations were generated, and all met the criteria.

The reservoir horizons are converted to depth using each velocity realisation, and then a small residual mistie correction is applied at the well locations. Reservoir characteristics are then calculated for each model. In this case, Gross Rock Volume (GRV) was the metric chosen to understand the impact of the different realisations and was calculated using two approaches. The first approach used the lowest closing contour being representative of a 4-way dip closure. The second approach calculated the GRV above a common free water level depth and is representative of a stratigraphic trap to the southeast. For the 4-way dip closure scenario, the realisations were ordered according to the depth of the lowest closing contour, and key realisations (P0, P10, ..., P100) identified. The data were migrated with these realisations and associated anisotropy models, giving an interpretable product. The reservoir horizons for these realisations can be seen in Figure 4. The probability maps in Figure 5 show what percentage of realisations have the given location within the reservoir for the two approaches used.

Conclusions

A robust depth uncertainty analysis was undertaken on data from the Petrel field, offshore Australia. The main goal of this study was to quantify the range of uncertainties for the depth of the reservoir across the field, particularly in the area of the structural spill point, towards the south-east of the field.

The results were used to derive a range of possible lowest closing contours, which could then be compared and validated against the range of free water level depths, interpreted from the well and dynamic data. Moreover, the impact of the structural uncertainties on the in-place volume of gas could be quantified.

Inconsistency between the most likely well-derived free water level and the P50 lowest closing contour estimated from this study has challenged the previous interpretation of a fully closing four-way dip closure as the main trapping mechanism for the field. It should however be noted that the shallow P90 Free Water Level case is similar to the P10 lowest closing contour case, and therefore a conventional structural trap remains a possibility constrained by physical data. These results have also been integrated into a larger geophysical work program, including spectral decomposition and the use of advanced AVA attributes. This was undertaken to better understand reservoir distribution and potential facies changes in the spill point area, which could support a possible stratigraphic component defining the trapping mechanism for the field.

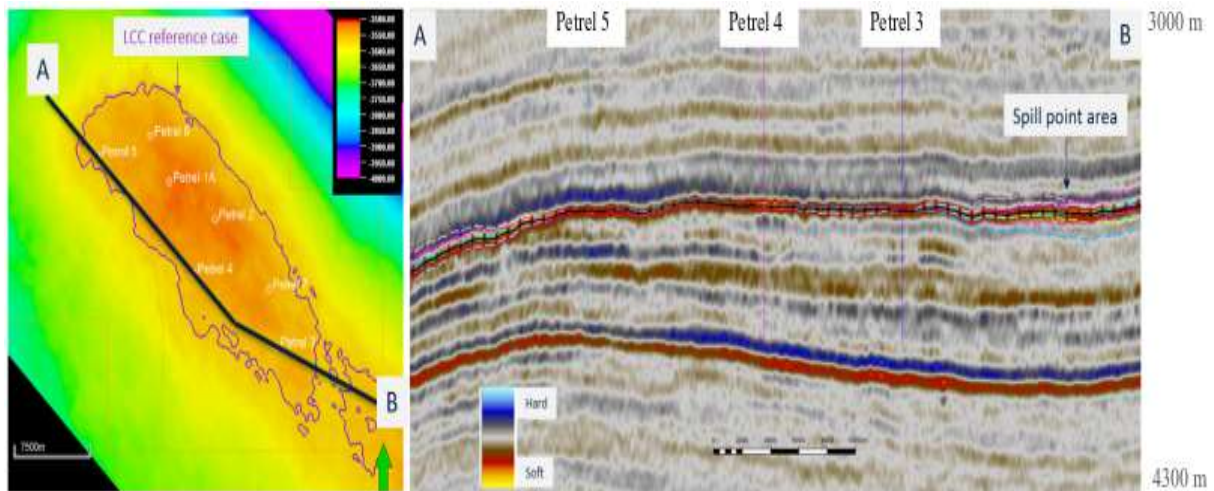


Figure 4 The top reservoir horizon is displayed for 11 key realisations, overlaid with the seismic stack for the given arbitrary line.

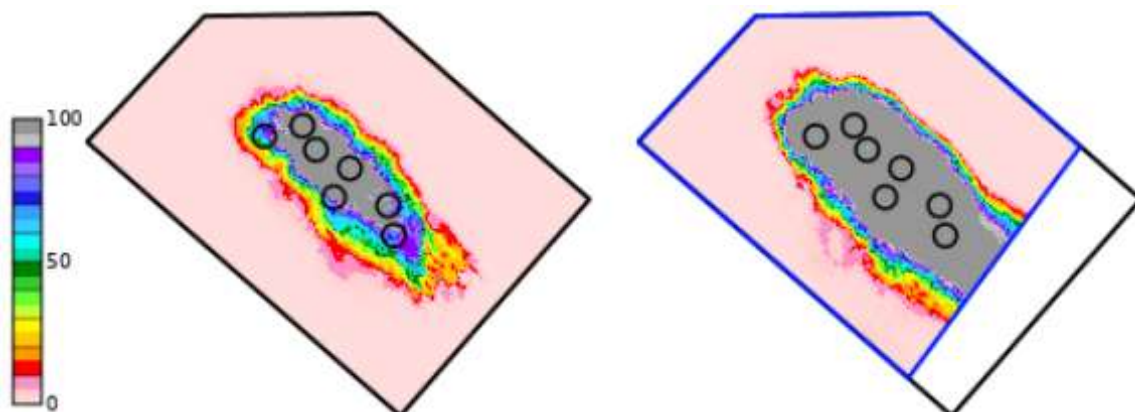


Figure 5 The probability (%) of a location being within the reservoir when using the lowest closing contour (left) and above a water contact within the blue polygon (right). Circles depict well locations.

Acknowledgements

Thanks to the Petrel field Joint Venture participants - Santos Limited and Beach Energy for their permission to share the details and results of the study.

References

- Cressie, N. A. [1993] *Statistics for Spatial Data*. John Wiley & Sons, New York
 Akkhalifa, T. and Tsvankin, I. [1995] Velocity analysis in transversely isotropic media. *Geophysics* **60**, 1550-1566.